



FORUM ACUSTICUM EURONOISE 2025

ACOUSTIC CHARACTERISTICS OF AN OPEN-FAN MODEL FROM SEMI-ANALYTICAL PREDICTIONS AND WIND-TUNNEL TESTS

C. Polacsek^{*1} V. Daydé-Thomas² S. Fauqueux¹

J. Mardjono² M. Descamps²

¹ ONERA, Institut Polytechnique de Paris, F-92322 Châtillon, France

² Safran Aircraft Engines, Moissy-Cramayel, 77550, France

ABSTRACT

This study investigates the ability of CFD coupled to semi-analytical methods to restitute the sound radiation from an open-fan designed by SAE (Safran Aircraft Engines) recently tested in S1-Modane wind tunnel. The acoustic predictions are restricted to sound sources located on the rotor blades and stator vanes. The tone noise is assessed using a source-mode integral formulation derived from the Ffowcs-Williams and Hawkings analogy written in the frequency domain and in which the harmonic loadings are issued from URANS calculations performed by SAE. A compact-source approach allowing quite fast calculations is also proposed. Broadband noise is estimated using analytical models derived from Amiet's theory with RANS-based inputs. Calculations are focused on take-off condition (sideline point), without incidence angle.

First results obtained for tone noise show a fairly good matching between fully non-compact and compact predictions and a reasonable agreement with measured sound directivities at BPF1 and BPF2, which should be presented during the Conference. Broadband noise assessment is still underway and present analyzes, at take-off condition too, are devoted to a previous generic open fan from SAE. ONERA predictions (using in-house tools) are found to be very close to SAE ones (from own industrial tool), in terms of both power spectra and overall sound pressure level directivities, when using common RANS inputs.

Keywords: Open Fan, noise predictions, wind tunnel tests

***Corresponding author:** cyril.polacsek@onera.fr

Copyright: ©2025 C. Polacsek et al. This is an open-access article distributed under the terms of the Creative Commons Attribution 3.0 Unported License, which permits unrestricted use, distribution, and reproduction in any medium, provided the original author and source are credited.

1. CONTEXT AND OBJECTIVES

The open-fan engine architecture developed through the CFM RISE program is mainly designed for short to medium-range flights, and aims to reduce fuel consumption by increasing the bypass ratio. Its fairing-free propeller and stator can be questionable for noise radiation to the ground, which leads to numerous research activities in view of acoustic certification. The present study, performed through a collaboration between ONERA and SAE (Safran Aircraft Engines), investigates the ability of CFD coupled to semi-analytical methods to restitute the sound radiation from an open-fan model, recently tested in S1-Modane wind tunnel. Although more advanced numerical simulations as the ones based on Lattice Boltzmann method are being explored, mid-fidelity approaches are still helpful for fast predictions at design stage or to assess representative sound characterization in addition to (or coupling to) microphone array processing. To this aim, a semi-analytical radiation tool (Python code) based on a source-mode integral formulation has been recently developed by ONERA in the framework of a PhD (funded by SAE). This propagation model is applied here for tone noise predictions, only focusing on rotor and stator blade sound sources in subsonic conditions. It has been also implemented (as a steering function) in an in-house source imaging technique (not discussed in the present work). Additional prediction models based on Amiet's theory are proposed and applied to estimate the broadband noise contributions generated by the propeller (self-noise) and the stator (interaction noise). The required inputs to these prediction methods are issued from CFD calculations performed and shared by SAE.

The paper is organized as follows. The open fan configuration, so-called "EcoEngine", is briefly presented in Section 2. Then the prediction methods (tone and broadband noise) are presented in Section 3 and the acoustic results are discussed in Section 4. Finally, some conclusions and perspectives are addressed in Section 5.



11th Convention of the European Acoustics Association
Málaga, Spain • 23rd – 26th June 2025 •





FORUM ACUSTICUM EURONOISE 2025

2. ECOENGINE CONFIGURATION

A test campaign named "EcoEngine", related to a 1/5.5 scale open fan engine designed by SAE, has been carried out in S1MA ONERA wind tunnel (located in Modane) during 2023 and 2024. The complete test matrix features high-speed and low-speed regimes, isolated and installed configurations, and angle of attack (incidence) effects. Assessment of aerodynamics performance and acoustic characteristics has been achieved using dedicated instrumentation. Low-speed isolated configurations considered in this paper were tested using an 8m-diameter rig equipped with acoustic treatment on the walls. A picture of the USF (Unducted Single Fan) model in the rig with two arms of near-field microphones is shown in Fig. 1. Several axial lines of wall-mounted microphones have been used to assess far-field directivities (in the range of about ± 6 meters) at different azimuthal positions.

The USF is made of a B-blade rotor and a W-vane (homogeneous) stator. The take-off condition (sideline certification point) is defined by a nominal (100%) rotation speed and for a flight Mach number equal to 0.29.



Figure 1. Picture of the open fan model with two arms of microphones and in S1MA wind tunnel

3. PREDICTION METHODS

3.1 Tone noise

3.1.1 Source-mode formulations (rotor and stator)

The tone noise prediction model is derived from the FW-H (Ffowcs Williams and Hawkings) analogy written in the frequency domain and by adopting a "source-mode" formalism [1]. Equations associated to the thickness noise (rotor) and loading noise (rotor and stator) terms are fully detailed in [1]. Only final expressions in a condensed form are given here:

$$p_T(x, \omega_{nB}) = \frac{B}{8\pi^2} \int_S \int_0^{2\pi} \rho_0 V_N \left[\frac{Mc_0(x - x_s)}{D^3} + i \frac{\omega_{nB}\sigma}{D^2} \right] e^{-i(k_{nB}\sigma + nB\theta)} dS d\theta \quad (1)$$

$$p_L(x, \omega_{nB}) = \frac{B}{8\pi^2} \int_S \sum_{k=-\infty}^{+\infty} F_{s=kW} \int_0^{2\pi} \frac{n\zeta}{D} e^{-i[k_{nB}\sigma + (nB-s)\theta]} dS d\theta \quad (2)$$

$$p'_L(x, \omega_{nB}) = \frac{W}{8\pi^2} \int_{S'} F_{s=nB} \sum_{k=-\infty}^{+\infty} \int_0^{2\pi} \frac{n\zeta}{D} e^{-i[k_{nB}\sigma + (s-kW)\theta]} dS' d\theta \quad (3)$$

In these equations, p_T and p_L respectively denote the thickness and loading noise, and superscript ' stands for the stator contribution. All the variables within the integrals are prescribed by geometry and kinematics except the harmonic loadings, F_s , which are the (unknown) inputs to be fed. The steady loading is retrieved by setting $s = 0$ in Eqn. (2). Tone noise predictions issued from these formulations have been validated on a generic open fan model using URANS-based inputs (see 3.1.3) by comparison with a trustworthy time-domain FW-H solver (KIM) [2,3].

3.1.2 Compactness approximation

A compact model (intended to microphone array processing) can be also considered by integrating the loadings (F_s) along the airfoil and projecting onto usual forces (the radial component being assumed negligible). The azimuthal lift (\mathcal{L}) and axial drag (\mathcal{D}) so obtained and applied at single (quarter-chord) position (ξ_{eq}) writes:

$$\mathcal{L}(\xi_{eq}) = dr \int_{-c/2}^{c/2} F_s(\xi) n_\theta(\xi) d\xi \quad (4)$$

$$\mathcal{D}(\xi_{eq}) = dr \int_{-c/2}^{c/2} F_s(\xi) n_x(\xi) d\xi \quad (5)$$

As discussed in [1], the initial span distribution can be also approximated by a sum of radial strips, allowing to practically reduce the surface sources (mesh cells) to about ten compacted sources. A satisfactory agreement between non-compact and compact solutions is shown in [1].

3.1.3 URANS-based inputs

URANS calculations have been performed by SAE using *elsA* code (ONERA-Safran property) [4], with a finite-volume approach and a K- ω Wilcox turbulence model. The CFD domain limited to a single channel thanks to a chorochronic approach counts about 35 million mesh cells. The loading harmonics F_s of order s are assessed from the time domain solution using a Fourier transform of the unsteady pressure $F(t)$, as:

$$F_s = \frac{\Omega}{2\pi} \int_0^{2\pi/\Omega} F(t) e^{-is\Omega t} dt \quad (6)$$

A 3D visualization of typical loading harmonics on the blade/vane surface of a generic open fan model issued from URANS data post-processing is shown in Fig. 2.





FORUM ACUSTICUM EUROTOISE 2025

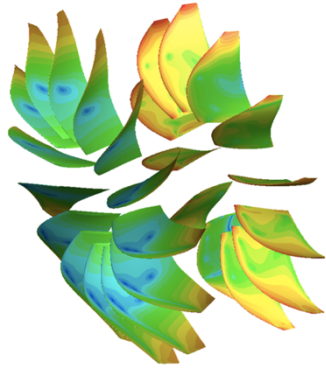


Figure 2. Iso-color level map (in dB) of pressure loading harmonic (BPF1) on rotor blade and stator vane surface (result from [3] for a generic open fan)

3.2 Broadband noise

3.2.1 Rotor self-noise

The rotor self-noise is achieved using ONERA code BABAR, used here to estimate the TBLTE (Turbulent Boundary Layer scattering from Trailing Edge) sound mechanism, although other secondary sources can be included following the work of Brooks et al. [5]. The present model is derived from original Amiet's one [6]:

$$S_{pp}(x, \omega) = \left(\frac{\omega z b}{\pi c_0 S_0^2} \right)^2 \frac{L}{2} \left| \mathcal{L} \left(\frac{\bar{\omega}}{U_c}, \bar{k} \frac{y}{S_0} \right) \right|^2 \Phi_{pp}(\omega) l_y(k \frac{y}{S_0}, \omega) \quad (7)$$

$$\frac{\Phi_{pp}(\omega)}{\rho_0^2 \delta^* U_e^3} = \frac{p_{ref}/2}{1 + \bar{\omega} + 0.217 \bar{\omega}^2 + 0.00562 \bar{\omega}^4}, \quad \bar{\omega} = \omega \delta^* / U_e$$

The wall pressure spectrum (Φ_{pp}) of Eqn. (7) can be improved by using Schinkler [7] or Rozenberg [8] models, and the main unknowns to be provided (from RANS) are the displacement thickness (δ) and the boundary layer outer velocity (U_e), extracted at 98% chord. The radial correlation lengthscale, l_y , is currently estimated using Corcos' model.

3.2.2 Stator interaction noise

Broadband interaction noise, due to the turbulent blade wakes impinging the stator vanes, is assessed using an in-house code (*TINA*) derived from Amiet's theory too [9]. The original isolated airfoil model has been extended to the open-fan annular cascade geometry taking into account for a stagger angle (δ_r). This updated formulation writes:

$$S_{pp}(\vec{x}, \omega) = \left(\frac{\rho_0 b}{S_0^2} \right)^2 U_c d\pi \Re(x, z, \delta_r) \left| L \left(x, K_c, \frac{ky}{S_0} \right) \right|^2 \Phi_{\xi\xi} \left(K_c, \frac{ky}{S_0} \right) \quad (8)$$

$$\Re(x, z, \delta_r) = k^2 z^2 \cos^2 \delta_r + k^2 \frac{(x^2 - M_x S_0)^2}{\beta^4} \sin^2 \delta_r + 2k^2 \frac{(x - M_x S_0)}{\beta^2} z \cos \delta_r \sin \delta_r$$

The radial evolution of the local geometry and turbulent inflow characteristics is achieved through a strip approach. The main inputs (provided by RANS) are the radial profiles of the turbulence intensity (TI) and turbulence length scale (TLS), used to fit the upwash turbulent velocity spectrum ($\Phi_{\xi\xi}$), adopting a standard von-Kármán spectrum model. These fields are obtained from CFD data extracted in a section plane aligned with the stator leading edge.

3.2.3 RANS-based inputs

RANS calculations only including the rotor have been performed too in order to provide the required inputs to the respective broadband noise models. TI values required as inputs for broadband interaction noise predictions are classically deduced from the turbulent kinetic energy (K , from $K-\omega$ Wilcox model). TLS value can be estimated by following Pope [10], giving rise to the expression denoted here Λ_p :

$$\langle \Lambda_p \rangle = \frac{C_{re}}{C_\mu} \frac{\sqrt{\langle k \rangle}}{\langle \omega \rangle} \quad (9)$$

C_{re} and C_μ are semi-empirical constants, practically set equal to 0.4 and 0.09 for turbofan applications. Another estimator is derived from the Ganz approach [11], relying on the blade wake characteristics i.e., the area (A_w) and the velocity deficit (d_w), assuming a gaussian shape. Ganz-based TLS, denoted Λ_g , writes:

$$\langle \Lambda_g \rangle = 0.2 \frac{A_w}{d_w} \quad (10)$$

Typical profiles of TI and TLS (adimensioned with respective maximum value) obtained using RANS-based data are plotted in Fig. 3.

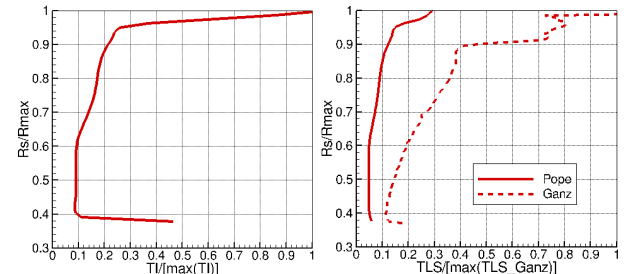


Figure 3. Radial profiles of turbulence characteristics: TI (left), Pope-based and Ganz-based TLS (right)





FORUM ACUSTICUM EURONOISE 2025

4. ACOUSTIC RESULTS

Acoustic results for tone and broadband noise at sideline conditions are discussed in this Section. Predictions related to EcoEngine configuration are restricted here to tone noise calculations (Section 4.1), whereas broadband noise analyzes (underway) should be discussed during the Conference. Broadband noise predictions in Section 4.2 are devoted to a SAE generic open fan geometry (INPRO project) previously studied and never presented yet. Cross-comparisons between ONERA and SAE (using own industrial tool *OPTIBRUI*, originally devoted to turbofan noise assessment [12,13]) solutions are addressed too.

A synchronous averaging is performed to split the tonal and broadband contributions, required for more reliable comparisons with respective predictions. Acoustic measurements from selected microphones obtained this post-treatment show a rather good emergence of the first tones above the broadband noise (partly polluted by the background noise and installation effects at low frequency). Tone noise analyzes are focused on BPF1 and BPF2, since mainly contributing to the overall spectrum level.

4.1 Tone noise

4.1.1 Predicted rotor and stator noise contributions

Predicted SPL directivities at 18 microphone positions of wall-mounted axial antenna (at 12 o'clock) are first analyzed and plotted for BPF1 and BPF2, in Figs. 4 and 5, respectively. Contributions from rotor sources (steady and unsteady loadings) and stator sources (unsteady loadings) are addressed separately, for fully non-compact and compact formulations. The expected variations in the azimuthal direction with a $2\pi/W$ periodicity [1,3] are assessed by calculating the radiated field on 8 duplicated axial lines (including the actual antenna) regularly spaced along this $2\pi/W$ sector. The curves in solid and dashed lines are displaying the mean SPL directivities (from non-compact and compact calculations) averaged over this sector. The level scales are the same for all figures, so that the balance between each contribution is clearly provided. A reasonable agreement between non-compact and compact solutions can be observed, which confirms the possibility to adopt a compact source-mode model for fast calculations (about 1 minute on a PC) and for microphone array processing as discussed in [1]. At BPF1 (Fig. 4), the SPL in the vicinity of the rotor plane ($x = 0$ m) is dominated by the rotor steady loading noise, whereas the stator noise is mainly contributing to the downstream radiation [-6 m, -2 m]. At BPF2 (Fig. 5), both steady and unsteady loadings contribute to the rotor noise with maximum SPL close to the stator one, giving rise to a flatter total directivity shape.

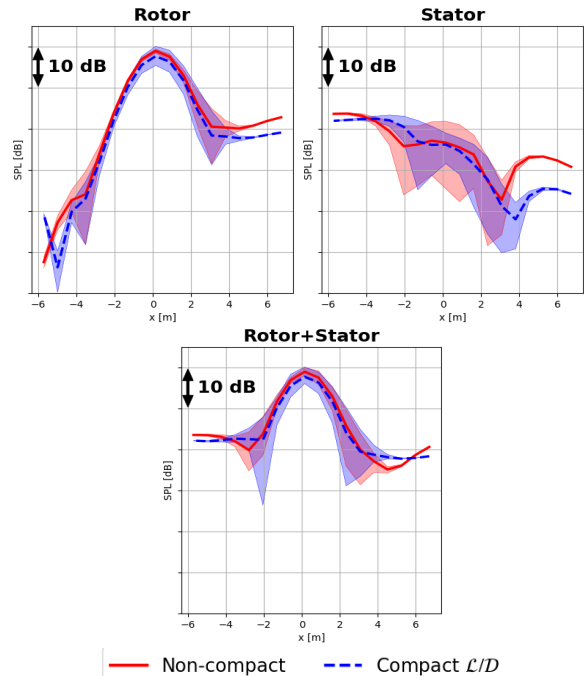


Figure 4. Predicted SPL directivities (upstream $x > 0$) at BPF1 issued from non-compact and compact formulations.

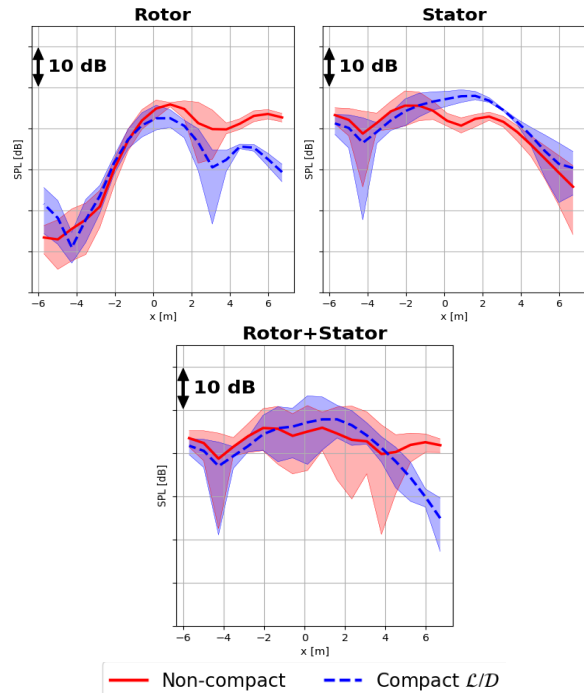


Figure 5. Predicted SPL directivities (upstream $x > 0$) at BPF2 issued from non-compact and compact formulations.





FORUM ACUSTICUM EURONOISE 2025

4.1.2 Comparisons with measurements

Preliminary qualitative comparisons with acoustic measurements from microphones of wall-mounted axial antenna are discussed here (these first results should be shown during the Conference). Despite stronger oscillations visible on the experimental directivities, the overall shape and levels of predicted directivities, at same azimuthal position than the selected antenna, are matching quite well the measurements in the axial range [-4m, 4m]. Significant deviations are observed for most upstream and downstream microphones, more particularly for BPF1. Spectrum analysis performed on these microphones, aiming at splitting the tonal and broadband contributions has evidenced that the expected tones were not actually found to emerge from the broadband part (close to the threshold of the wind tunnel background noise). This probably explains this mismatch at the sides of the antenna. The main trends from rotor and stator predictions discussed in Section 4.1.1, showing that the steady loading from the rotor is mainly contributing to the total noise (around the rotor plane) at BPF1, whereas rotor and stator contributions are balanced at BPF2, are confirmed by the experiment.

4.2 Broadband noise (INPRO case)

4.2.1 Rotor self-noise

The rotor-self noise has been assessed using RANS inputs from SAE feeding the acoustic code *BABAR*. The wall pressure spectrum is estimated using the Schinkler and Rozenberg models, and the radial correlation length scale is derived from Corcos's model. ONERA predictions are compared to *OPTIBRUI* solution (using Rozenberg model). PWL spectra and OASPL directivities for a circular antenna at 45 meters from the rotor center are plotted in Fig. 6, top and bottom, respectively. Schinkler-based power spectrum predictions show a higher level at lower frequencies and a stronger attenuation slope compared to the one obtained with Rozenberg model. OASPL directivities are found rather close for both models. A very nice agreement can be observed between ONERA and SAE solutions with identical Φ_{pp} model (Rozenberg here).

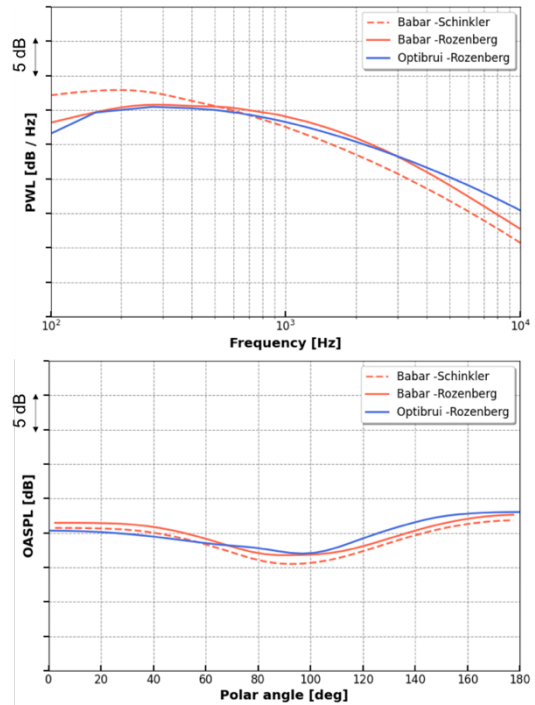


Figure 6. BBN predictions provided by ONERA (*BABAR*) and compared to SAE solution (*OPTIBRUI*): PWL spectra (dB/Hz, top) and OASPL directivities on a circular antenna (0° upstream) at 45 meters (bottom)

4.2.2 Stator interaction noise

A similar benchmark has been performed for stator interaction noise using *TINA* code, recently adapted for open fan applications. The RANS-based radial profiles of TI and TLS used as inputs for these calculations are those shown in Fig. 3. The assessment of TI derived from the turbulent kinetic energy provided by RANS is rather well defined and reasonable deviations should be expected from usual 2-equation turbulence models. On the other hand, the estimation of a reliable TLS is more challenging, in particular for these new USF architectures, for which parametric studies and benchmarking as done for turbofans [14] are missing. The TLS profiles in Fig. 3 estimated using Pope and Ganz approaches, commonly adopted in turbofan applications, reveal significant differences, trimming the stator noise predictions. Results are displayed in Fig. 7, in which PWL spectrum and OASPL directivity provided by *TINA* and *OPTIBRUI* are matching quite well (when iso-inputs for turbulence profiles are used), which makes these predictions (from two different codes) more confident. As expected from Fig. 3, large level differences can be observed when using Pope-





FORUM ACUSTICUM EUROTOISE 2025

based TLS, and experimental results should help to set the good practices to fit the main trends.

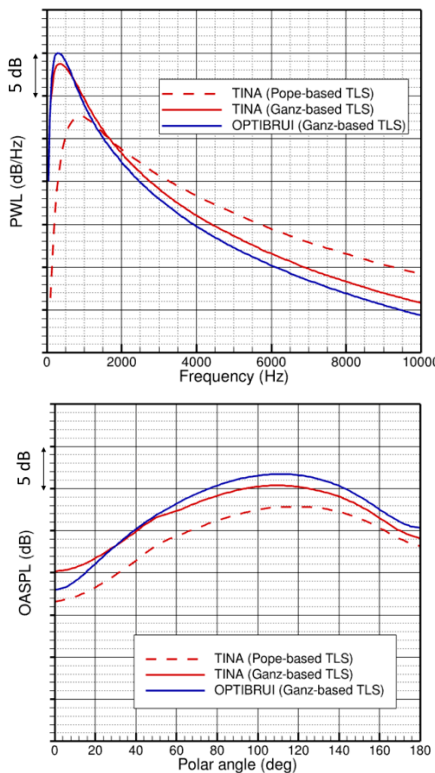


Figure 7. BBN predictions provided by ONERA (*TINA*) and compared to SAE solution (*OPTIBRUI*): PWL spectra (dB/Hz, top) and OASPL directivities on a circular antenna (0° upstream) at 45 meters (bottom)

5. CONCLUSIONS

Tone noise and broadband noise predictions related to open fan engines designed by SAE have been discussed in this paper, focusing on take-off operating point. At this regime, dominant sound radiation is expected to be mainly generated by dipolar sources from rotor blade and stator vanes, so that usual approaches derived from FW-H analogy and Amiet's theory can be adopted, for tonal and broadband noise assessment, respectively. Tone noise calculations have been applied to an open fan model recently tested in S1MA wind tunnel (EcoEngine test campaign), while broadband noise analyzes are focused on a previous generic USF (results never presented), application to EcoEngine case being still underway.

SPL directivities obtained by using the FWH analogy written through a source-mode formulation (Python code), for which loading harmonics are provided by URANS

chorochronic calculations with ONERA-SAE *elsA* solver, are found to match rather well the experimental ones at BPF1 and BPF2 (quantitative results should be presented during the Conference). For the broadband noise assessment, rotor-self noise and stator interaction noise contributions, predicted by using respective Amiet-based in-house ONERA tools, have been compared to SAE solutions issued from the code *OPTIBRUI* (currently used by SAE). A fairly nice agreement in terms of PWL spectra and OASPL directivities have been shown when using common RANS-based inputs. First comparisons with EcoEngine tests should be presented during the Conference too.

6. ACKNOWLEDGMENTS

This work was partly performed within the funding of Safran Aircraft Engines, through funds from the Association Nationale de la Recherche et de la Technologie (ANRT) and the French DGAC project MAMBO. The authors thank Masakazu Sugiyama (PhD student, Safran Aircraft Engines) for its contribution to the broadband calculation results in Section 4.2.

7. REFERENCES

- [1] V. Daydé-Thomas, C. Polacsek, S. Fauqueux, X. Gloerfelt, J. Mardjono, "Tone noise characterization of an open-fan engine using source-mode integral formulation," 30th AIAA/CEAS Aeroacoustics Conference, Roma (Italy), 2024.
- [2] J. Prieur, and G. Rahier, "Aeroacoustic integral methods, formulation and efficient numerical implementation," Aerospace Science and Technology, Vol. 5, No. 7, pp. 457–468, 2001.
- [3] M. Sugiyama, N. Jaouani, F. Falissard, G. Reboul, and X. Gloerfelt, "Numerical investigation of Open Fan's tonal noise prediction in low and high-speed condition," 30th AIAA/CEAS Conference 2024, Roma (Italy), 2024.
- [4] L. Cambier, S. Heib, and S. Plot, "The Onera *elsA* CFD software: input from research and feedback from industry," Mechanics & Industry, Vol. 14, No. 3, 2013, pp. 159–174.
- [5] T. F. Brooks, D. S. Pope et M. A. Marcolini, "Airfoil self-noise and prediction," NASA RP 1218, 1989.





FORUM ACUSTICUM EURONOISE 2025

- [6] R. K. Amiet, "Noise due to turbulent flow past a trailing edge," *Journal of Sound and Vibration*, Vol. 74(3), pp 387-393, 1976.
- [7] R. Schlinker, and R. Amiet, "Helicopter rotor trailing edge noise," 7th Aeroacoustics Conference, 1981, p. 2001.
- [8] Y. Rozenberg, G. Robert, and S. Moreau, "Wall-pressure spectral model including the adverse pressure gradient effects," *AIAA journal*, Vol. 50, No. 10, pp. 2168–2179, 2012.
- [9] R. K. Amiet, "Acoustic Radiation from an Airfoil in Turbulent Stream," *J. Sound Vib.*, 41(4), pp. 407–420, 1975.
- [10] S. B. Pope, "Turbulent Flows," Cambridge Univ. Press, England, U.K., 2000.
- [11] U. W. Ganz, P. D. Joppa, T. J. Patten, and D. F. Scharpf, "Boeing 18-Inch Fan Rig Broadband Noise Test," NASA report, CR-1998-208704, 1998.
- [12] H. Posson, S. Moreau, M. Roger, "Broadband noise prediction of fan outlet guide vane using a cascade response function," *J. Sound Vib.*, 330, 6153–6183, 2011.
- [13] J. de Laborderie, "Approches Analytiques et Numériques pour la Prédition du Bruit Tonal et Large Bande de Soufflantes de Turboréacteurs", Ph.D Thesis, Université de Sherbrooke, QC, Canada, 2013.
- [14] C. Kissner, S. Guérin, P. Seeler, M. Billson, P. Chaitanya, P. C. Larana, H. de Laborderie, et al., "ACAT1 Benchmark of RANS-Informed Analytical Methods for Fan Noise Prediction: Part I—Influence of the RANS Simulation," *Acoustics*, 2(3), pp. 539–578, 2020.

